VIP Contact Electrification Very Important Paper

DOI: 10.1002/anie.201307249

Water-Solid Surface Contact Electrification and its Use for Harvesting Liquid Wave Energy**

*Zong-Hong Lin, Gang Cheng, Long Lin, Sangmin Lee, and Zhong Lin Wang**

Contact electrification, also called triboelectrification, is an old but well-known phenomenon in which surface charge transfer occurs when two materials are brought into contact. Although some of the fundamental mechanisms about triboelectrification are still under discussion, such as what subjects (electrons, ions, or small amounts of material) are transferred during the contact and separation process to produce the charged surface,[1,2] and why surface charge transfer occurs even between identical materials,[3] triboelectrification does exist and it has some practical applications together with many negative consequences. Recently, contact electrification has been demonstrated for some potential applications, such as energy harvesting,[4] chemical sensors,[5,6] electrostatic charge patterning,[7,8] metal-ion reduction,[9–11] and laser printing.[12]

The triboelectric nanogenerator (TENG),[4] which is the first invention utilizing contact electrification to efficiently convert mechanical energy into electricity, has been systematically studied to instantaneously drive hundreds of light-emitting diodes (LEDs)[13] and charge a lithium-ion battery for powering a wireless sensor and a commercial cell phone.[14] Recently, the research has been broadened to collect energy from environment, such as wind[15] and human motion,[16] under which the TENG works in relatively dry conditions, because the surface triboelectrification would be greatly decreased if not totally eliminated by the presence of water. However, water vapor and liquid water are abundant and the most obvious example is ocean waves and tides that have huge amounts of mechanical energy, which is inexhaustible and not largely dictated by daytime, season, weather and climate, in contrast to solar energy.[17]

Until now, TENG is designed to work between solid materials and works best under dry conditions.[4,13–16] However, tribolelectricity does exist when liquids are flowing through insulating tubes.[18–21] For example, a voltage variation rising up to 300 mV is observed when deionized water flows through a 1 m-long rubber tube.[20] Or a surface charge density of 4.5 $\mu C m^{-2}$ is measured on each water droplet pipetted from a polytetrafluoroethylene (PTFE) tip.[21] Therefore, herein we explore the opportunity to use water contact as one type of "material" choice for TENG. We demonstrate that the contact electrification between water and insulating polymer films can also be useful for TENG, which can derive a new application of TENG especially in liquid environments for sensing.

Polydimethylsiloxane (PDMS) and PTFE are chosen in this study for their hydrophobic properties and high negativity in the triboelectric series.[22,23] To further investigate this effect, TENGs using tap water, deionized water, and deionized water with a high concentration of NaCl are also compared. Under periodic contacting deionized water by a linear motor, PDMS film with patterned pyramid array can provide an open-circuit voltage (V_{oc}) of 52 V and short-circuit current density (J_{sc}) exceeding 2.45 $mA m^{-2}$ with a peak power density of nearly 0.13 $W m^{-2}$, which is large enough to light up 60 commercial LEDs. The incubation shaker and platform rocker are used to stimulate different wave motions in the environment and the water–TENG successfully harvests these types of mechanical energy into electricity. Moreover, the water–TENG also has the capability to act as a chemical and temperature sensor.

Figure 1 shows the fabrication process of the TENG and how the water contact electrification is included in the action unit. The TENG fabrication starts from the design of a PDMS film with patterned pyramid array (Figure 1a). The Si wafer mold was made by photolithography and then etched by a dry etching process. Liquid PDMS elastomer and cross-linker were mixed, degassed, and uniformly spin-coated on the Si wafer mold. After thermal incubation, a uniform PDMS film with a patterned pyramid array was formed. For the other part of the construct, thin films of Cu (100 nm) were deposited on two poly(methyl methacrylate) (PMMA) substrates by a RF magnetron sputtering deposition system. PMMA is selected as the substrate material because it provides a flat surface, light weight, and high strength. The PDMS film with the pyramid array pattern was peeled off the Si wafer mold and then placed on one of the Cu thin-film-deposited PMMA substrates with uncured PDMS mixture on top. Finally, the structure was incubated again to obtain a fully developed device for use in the next step.

To investigate the contact electrification between water and the PDMS film, the second Cu thin-film-deposited PMMA substrate was placed on the bottom of an insulating tank (Figure 1b), acting as the conducting electrode for the water. The dimensions of the tank were 11 cm × 7 cm. After the tank was filled with water, the device consisting of the

[*] Dr. Z.-H. Lin, Dr. G. Cheng, L. Lin, Dr. S. Lee, Prof. Z. L. Wang
School of Material Science and Engineering
Georgia Institute of Technology
Atlanta, GA 30332-0245 (USA)
E-mail: zlwang@gatech.edu
Prof. Z. L. Wang
Beijing Institute of Nanoenergy and Nanosystems
Chinese Academy of Sciences, Beijing (China)

[**] This work was supported by Airforce, MURI, U.S. Department of Energy, Office of Basic Energy Sciences (DE-FG02-07ER46394), NSF, and the Knowledge Innovation Program of the Chinese Academy of Sciences (KJCX2-YW-M13).

Supporting information for this article is available on the WWW under http://dx.doi.org/10.1002/anie.201307249.

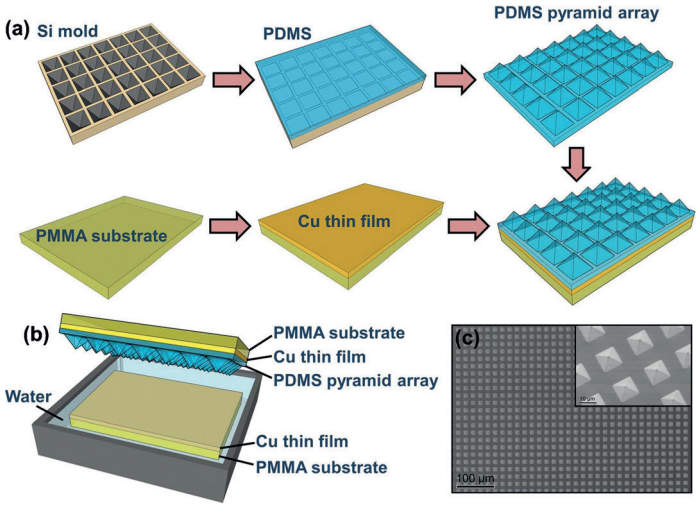

Figure 1. a) Fabrication process of patterned PDMS pyramid array and related device. b) Schematic diagram of the water-based TENG. c) SEM image of patterned PDMS pyramid array. Inset is an SEM image with higher magnification.

patterned PDMS pyramid array was controlled by a linear motor to periodically make contact with the water and then separate. The depth of water layer is 2 cm. During the contact electrification process, the PDMS film only made contact with the water surface and did not touch the Cu thin-film-deposited PMMA substrate on the bottom of the tank. Figure 1c displays scanning electron microscopy (SEM) images of the patterned PDMS pyramid array, showing uniform microstructures distributed across the whole area. The thickness of PDMS film is nearly 140 μm (Figure S1 in the Supporting Information). These microstructures not only act as steady gaps between two contact materials in a strain-free condition, but also enable the contact area of two materials to be enlarged, which will increase the electrical output of the water–TENG. High-magnification SEM image (inset of Figure 1c) further reveals that the size of single pyramid is 10 μm, and each pyramid has a perfect geometric structure and a sharp tip.

Figure 2 illustrates the contact electrification between water and PDMS and the working mechanism of the water–TENG, which can be explained as a result of contact electrification and electrostatic induction. Before PDMS contacting with water (Figure 2a), no charge transfer occurred. When PDMS is forced into contact with water (Figure 2b), the ionization of the surface groups on the PDMS will cause the PDMS to be negatively charged[21,24] and create a positively charged electrical double layer (EDL) on the surface of the water to maintain electrical neutrality.[25] As the PDMS moves off the water, the positive charges in the EDL can be carried away with the water and the negative charges can remain on the surface of PDMS, then an electric potential difference will be established between PDMS and water. In the ideal situation, the PDMS can be completely separated from water leaving no residual water on the PDMS, generating the maximum electricity output. This is why we choose hydrophobic polymer materials, especially with the design of surface micro-patterns. In short-circuit case, the electrons will transfer from Cu electrode 2 to Cu electrode 1 through the external load to balance the potential difference between water and PDMS (Figure 2c). This contributes to the instantaneously positive current. The inducted charge density (σ'), which determines the magnitude of the generated current, has been shown to be highly dependent on the separated distance (d').[26] The maximum value of σ' is observed when PDMS returning to its original position ($d' = d_3$) (Figure 2d). Once PDMS is pressed again toward the water surface, the electric potential difference starts to decrease as the PDMS gets closer to the water (Figure 2e). Therefore, the electrons will flow from Cu electrode 1 to Cu electrode 2 through the external load, until achieving a new equilibrium (Figure 2b). This process corresponds to an instantaneous negative current. Once the PDMS is periodically making contacting with the water (Figure 2b–d), a continuous output will be obtained.

We first measured the electrical output of the water–TENG through the contact electrification between the patterned PDMS pyramid array and deionized water.

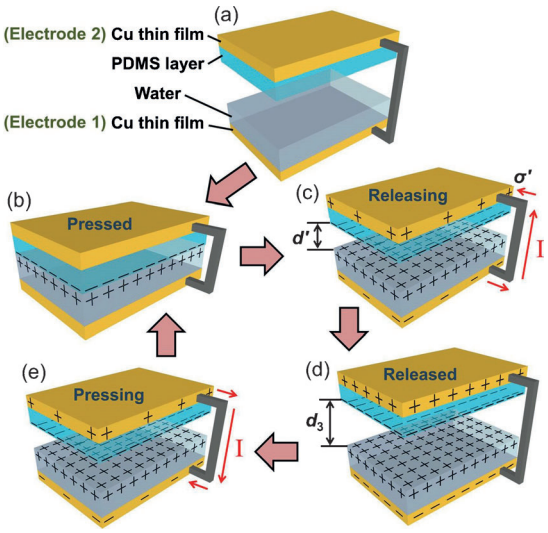

Figure 2. Working mechanism of the water–TENG. a) Initial status without any external force applied. b) External force brings the PDMS layer into contact with water. c) Removing the PDMS layer from the water surface. d) PDMS layer returning back to the original position. e) External force applied makes the PDMS layer contact with water again. For simplification, both PMMA substrates are not shown.

The TENG was mechanically triggered by a linear motor that provides dynamic impact with controlled force at a frequency of 2 Hz. V_{oc} and J_{sc} were measured separately to characterize the electrical performance of the water–TENG. From Figure 3a, the V_{oc} of the water-TENG surged from 0 to 82 V upon removing the patterned PDMS pyramid array from the deionized water surface to a separation distance of 1.5 cm. The generated voltage held as a plateau because in an open circuit the electrons cannot flow to screen the electric potential difference between patterned PDMS pyramid array and the deionized water (inset of Figure 3a). When

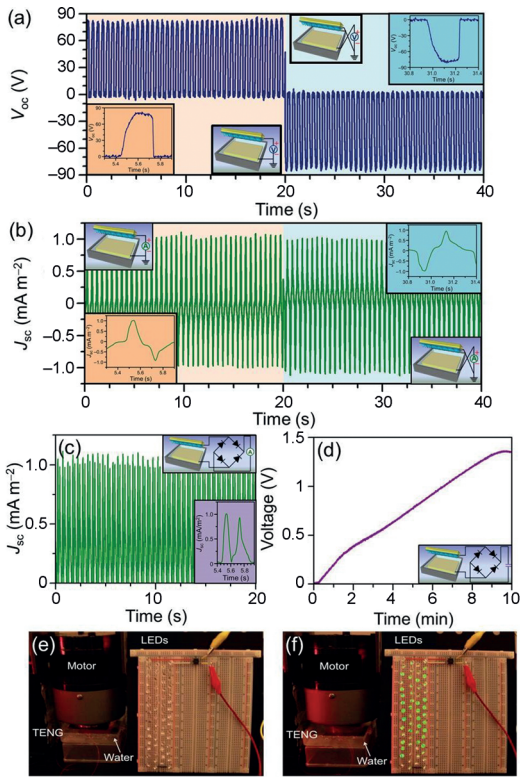

Figure 3. a) V_{oc} and b) J_{sc} of the water-TENG under a constant external force with a frequency of 2 Hz. Measurements operated both at the forward connection, shown at the left-hand side, and the reversed connection, shown at the right-hand side. c) The AC output transformed into a pulse output in the same direction by a full-wave rectifying bridge. d) The rectified output used to charge a capacitor. The insets are the magnified output curve in one cycle (a–c) and a diagram of the corresponding connection polarity (a–d). e) Photograph of a setup in which the water-TENG acts as a direct power source for 60 commercial green LED lamps and f) when the patterned PDMS pyramid array is in contact with the water, the LEDs light up.

the PDMS pyramid array moving back into contact with deionized water again, the V_{oc} fell back to 0.

In the short-circuit case, the charges transferred between Cu electrode 1 and Cu electrode 2 (Figure 2) in the external circuit during the contact and separation between the PDMS film and the water surface instantaneously generated positive and negative currents. The peak value of the J_{sc} reaches 1.05 mA m^{-2} (Figure 3b). The integration of positive and negative current peaks represents the transferred charges in releasing and pressing movements (Figure S2). Both the generated V_{oc} and J_{sc} exhibit corresponding reversed signs when the connection polarity to the electrometer is switched, indicating that the measured signals were generated by the water-TENG. The patterned pyramid array is effective for enhancing the output. Without the microstructures, the J_{sc} of PDMS film decreases to 0.3 mA m^{-2} (Figure S3), which is even smaller than that of a commercial PTFE sheet (Figure S4). Furthermore, the AC output could be transformed to a pulse output in the same direction simply by using full-wave rectifying bridge (Figure 3c) and stored in a capacitor of 33 μF (Figure 3d). With such a power output generated from water-contact electrification, 60 commercial LEDs can be instantaneously driven by a single water–TENG device (Figure 3e, Figure 3f, and Supporting Information Video S1).

As this model differs from the solid-material-based TENGs, we need to consider how the wave surface of water disturbs the contact areas with the PDMS, which consequently affects the generated output current. Actually, the movement of the PDMS film contacting and separating from water will generate a water wave. By changing the contact frequency of the linear motor, water waves with different wavelengths are created. The size of the tank could be critical. Therefore, the dependence between generated output and contact frequency was studied. Figure 4a displays that the generated J_{sc} decreased from 1.05 mA m^{-2} to 0.46 mA m^{-2} first as the contact frequency changing from 2 Hz to 3 Hz, then increased to 1.34 mA m^{-2} and 2.45 mA m^{-2} when the contact frequency altering from 4 Hz to 5 Hz, respectively. We found the dependence between J_{sc} and contact frequency is unlike that in solid-material-based TENGs,[27,28] in which, the generated J_{sc} keeps increasing with the increasing contact frequency, because the contact areas are fixed even with the change of contact frequency. Increasing the contact frequency only causes a higher flow rate of charges in the external circuit, but the total amount of charges transferred remains constantly. However, in the case of the water–TENG, the movement of the PDMS film controlled by the linear motor will create waves on the water surface, which in turn will disturb the contact area between the PDMS film and water. Hence the J_{sc} generated will not be solely dependent on the contact frequency. This can be further explained by the generated V_{oc} (Figure 4b), which is determined by the triboelectric charge density in the open-circuit condition.[4] The V_{oc} of a solid-material-based TENGs is not affected by the contact frequency.[14] But in the case of the water–TENG, the generated V_{oc} decreased from 82 V to 23 V, 45 V, and 52 V as the contact frequency changing from 2 Hz to 3 Hz, 4 Hz, and 5 Hz, respectively. The tendency explicitly shows that the triboelectric charge density in the water-TENG is influenced by the motions of water wave.

We measured the electrical output of the water–TENG upon connecting directly to loads of different resistances at a contact frequency of 5 Hz. As shown in Figure 4c, when the resistance is below 0.1 MΩ, the voltage remains close to 0 and the current density has only little changes. When the resistance is raised from 0.1 MΩ to 1 GΩ, the voltage through the load will generally increase, but the current across the load will decrease. Consequently, the instantaneous power density on the load (Figure 4d) remains small with the resistance below 0.1 MΩ and reaches the maximum value of nearly 50 mW m^{-2} at a resistance of 88 MΩ. This is the maximum output power density on this water–TENG.

To demonstrate the concept of the water–TENG which can be used to harvest energy from the environment, tap water and deionized water with high concentration of NaCl are also evaluated (Figure 4e,f, and S5). The concentration of NaCl (0.6 M) tested is similar to that in sea water. The J_{sc} generated decreases first and then increases as the contact frequency is varied from 2 Hz to 5 Hz, which is the same tendency as that of deionized water (Figure 4e). The maximum generated J_{sc} from tap water and 0.6 M NaCl solution

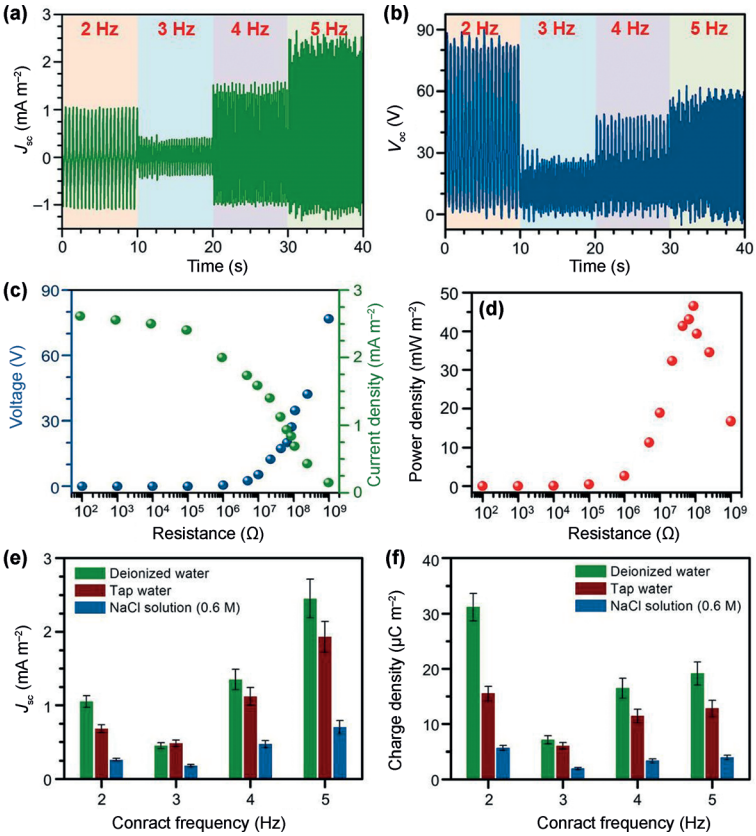

Figure 4. a), b) Influence of contact frequency between patterned PDMS pyramid array and deionized water on the a) J_{sc} and b) V_{oc} generated by the water-TENG. c),d) Dependence of output voltage (c), output current density (c), and output power density (d) of the water–TENG on the resistance of the external load. e),f) Comparison of e) J_{sc} and f) charge density generated from the contact electrification between different types of water and the patterned PDMS pyramid array. A different contact frequency was applied to evaluate the electrical output.

are 1.85 mA m^{-2} and 0.73 mA m^{-2} at a contact frequency of 5 Hz, respectively, which are 76% and 30% of that for the deionized water–TENG. By integrating the peak of J_{sc}, we can obtain the transferred charge density ($\Delta\sigma$) in each type of water (Figure 4 f). The results show the deionized water can provide the largest $\Delta\sigma$ of 31.3 μC m^{-2}. The $\Delta\sigma$ of tap water and 0.6 M NaCl solution TENGs are 15.02 μC m^{-2} and 5.7 μC m^{-2}, respectively, smaller than that of deionized water–TENG. The results indicate the output of the water-TENG will be affected by the electrolytes in water. This is because the PDMS film cannot be completely eliminated from the adhesion of water droplets after it is separated from the water. Once there are electrolytes in water, more positive charges including dissolved ions will remain on the films, resulting in a partial screening of the tribo-charges on the PDMS film.[21,24] Therefore, smaller electrical outputs than that in deionized water will be obtained. Although at the present time the electrical output of the water-TENG will be affected when electrolytes are present in water, this could be overcome in the future by designing the polymer surface to be superhydrophobic and/or modifying the polymer with specific functional group to eliminate the ions with opposite charges adsorbed onto the contacted surfaces. As a potential application of water–TENG, we used the fluctuating wave on surface to generate a wave controlled contact and separation process between the water surface and PDMS film for harvesting wave energy (Figure S6 and S7).

Finally, we demonstrated that the water-TENG can also be used as chemical and temperature sensors. The generated J_{sc} of the water-TENG decreased from 1.05 mA m^{-2} to 0.32 mA m^{-2} as the ethanol percentage by volume increase to 15% (Figure 5 a). The decrease in J_{sc} probably comes from the mixing with ethanol decreasing the water polarity. Previous study has verified that the dielectric constant and water polarity will decrease in the presence of less polar solvent, such as ethanol.[29] Therefore increasing the ethanol concentration in the mixture of water and ethanol will enhance the interaction with hydrophobic PDMS film, and consequently reducing the triboelectric charge density and generated output during the separation process. To clarify this point, the J_{sc} values of the water-TENG operating at different water temperatures were compared. Temperature has been studied as other key factor to affect the dielectric constant and polarity of water.[30] A similar tendency between water temperature and generated output was observed (Figure 5 b). From 25 °C to 75 °C, the J_{sc} value decreased from 1.05 mA m^{-2} to 0.28 mA m^{-2}. These two results indicate that the water–TENG can be applied to detect substances that will change the dielectric constant and/or polarity of water. In the future, the sensing system can be improved by growing nanomaterials or functionalizing specific molecules onto the surface of polymer films, which will serve as probes to selectively detect the targets in the solution samples. Once the probes catch the targets, the electrical output generated from the contact electrification with water will be different. This will be a better strategy in a water–TENG-based sensing system because it can directly change the triboelectric charge density upon detecting targets.

In summary, we have demonstrated a newly designed TENG based on the contact electrification between a patterned PDMS pyramid array and water. This new prototype water–TENG provided an open-circuit voltage of 52 V and a short-circuit current density of 2.45 mA m^{-2} with a peak power density of nearly 0.13 W m^{-2}, which is able to drive 60 LEDs simultaneously. The dependence of the electrical outputs on the contact frequency and motions of water waves has been systematically studied. Tap water and deionized water with a similar ion concentration to sea water were also evaluated and showed the potential for harvesting water-related energy from the environment. Compared with traditional TENGs that are designed for the contact of solid materials, this study opens the possibility in utilizing liquid movements and extends its application scope. Furthermore, we believe the electrical output of the water–TENG could be enhanced in the future by using superhydrophobic nanostructures as the contact materials or functionalizing material

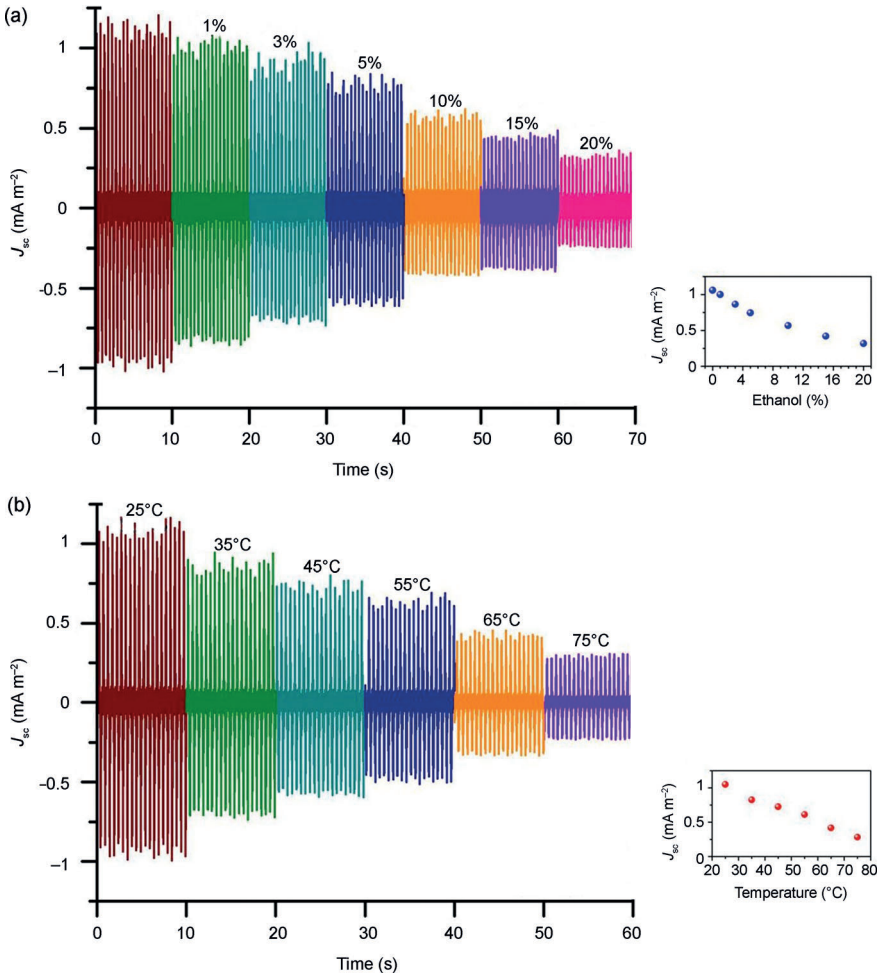

Figure 5. a) J_{sc} generated by the water–TENG in the presence of different percentage ethanol by volume. b) J_{sc} generated by the water–TENG upon working at different water temperatures. The measurements were conducted under a constant external force with a frequency of 2 Hz.

surface with specific groups. This work will also inspire the development of TENG toward directly sensing metal ions and biomolecules in solution samples.

Received: August 18, 2013
Published online: ■■ ■■, ■■■■

Keywords: contact electrification · sustainable chemistry · nanosensor · triboelectric nanogenerator · wave energy

[1] H. T. Baytekin, A. I. Patashinskii, M. Branicki, B. Baytekin, B. A. Grzybowski, *Science* **2011**, *333*, 308 – 312.
[2] D. J. Lacks, R. M. Sankaran, *J. Phys. D* **2011**, *44*, 453001.
[3] M. M. Apodaca, P. J. Wesson, K. J. M. Bishop, M. A. Ratner, B. A. Grzybowski, *Angew. Chem.* **2010**, *122*, 958 – 961; *Angew. Chem. Int. Ed.* **2010**, *49*, 946 – 949.
[4] F.-R. Fan, Z.-Q. Tian, Z. L. Wang, *Nano Energy* **2012**, *1*, 328 – 334.
[5] Z.-H. Lin, G. Zhu, Y. S. Zhou, Y. Yang, P. Bai, J. Chen, Z. L. Wang, *Angew. Chem.* **2013**, *125*, 5169 – 5173; *Angew. Chem. Int. Ed.* **2013**, *52*, 5065 – 5069.
[6] Z.-H. Lin, Y. Xie, Y. Yang, S. Wang, G. Zhu, Z. L. Wang, *ACS Nano* **2013**, *7*, 4554 – 4560.
[7] X. Ma, D. Zhao, M. Xue, H. Wang, T. Cao, *Angew. Chem.* **2010**, *122*, 5669 – 5672; *Angew. Chem. Int. Ed.* **2010**, *49*, 5537 – 5540.
[8] D. Zhao, L. Duan, M. Xue, W. Ni, T. Cao, *Angew. Chem.* **2009**, *121*, 6827 – 6831; *Angew. Chem. Int. Ed.* **2009**, *48*, 6699 – 6703.
[9] C. Y. Liu, A. J. Bard, *Nat. Mater.* **2008**, *7*, 505 – 509.
[10] C. Y. Liu, A. J. Bard, *J. Am. Chem. Soc.* **2009**, *131*, 6397 – 6401.
[11] B. Baytekin, H. T. Baytekin, B. A. Grzybowski, *J. Am. Chem. Soc.* **2012**, *134*, 7223 – 7226.
[12] D. M. Pai, B. E. Springett, *Rev. Mod. Phys.* **1993**, *65*, 163 – 211.
[13] G. Zhu, Z.-H. Lin, Q. Jing, P. Bai, C. Pan, Y. Yang, Y. Zhou, Z. L. Wang, *Nano Lett.* **2013**, *13*, 847 – 853.
[14] S. Wang, L. Lin, Z. L. Wang, *Nano Lett.* **2012**, *12*, 6339 – 6346.
[15] Y. Xie, S. Wang, L. Lin, Q. Jing, Z.-H. Lin, S. Niu, Z. Wu, Z. L. Wang, *ACS Nano* **2013**, *7*, 7119 – 7125.
[16] P. Bai, G. Zhu, Z.-H. Lin, Q. Jing, J. Chen, G. Zhang, J. Ma, Z. L. Wang, *ACS Nano* **2013**, *7*, 3713 – 3719.
[17] G. W. Taylor, J. R. Burns, S. M. Kammann, W. B. Powers, T. R. Welsh, *IEEE J. Oceanic Eng.* **2001**, *26*, 539 – 547.
[18] A. J. Morin, M. Zahn, J. R. Melcher, *IEEE Trans. Ind. Applicat.* **2005**, *41*, 1335 – 1342.
[19] T. Paillat, G. Touchard, *J. Electrost.* **2009**, *67*, 326 – 334.
[20] B. Ravelo, F. Duval, S. Kane, B. Nsom, *J. Electrost.* **2011**, *69*, 473 – 478.
[21] D. Choi, H. Lee, D. J. Im, I. S. Kang, G. Lim, D. S. Kim, K. H. Kang, *Sci. Rep.* **2013**, *3*, 2037.
[22] A. F. Diaza, R. M. Felix-Navarro, *J. Electrost.* **2004**, *62*, 277 – 290.
[23] L. S. McCarty, G. M. Whitesides, *Angew. Chem.* **2008**, *120*, 2218 – 2239; *Angew. Chem. Int. Ed.* **2008**, *47*, 2188 – 2207.
[24] B. J. Kirby, E. F. Hasselbrink, Jr., *Electrophoresis* **2004**, *25*, 187 – 202.
[25] J. Lyklema, *Fundamentals of Interface and Colloid Science*, Academic Press, New York, **1995**.
[26] G. Zhu, C. Pan, W. Guo, C.-Y. Chen, Y. Zhou, R. Yu, Z. L. Wang, *Nano Lett.* **2012**, *12*, 4960 – 4965.
[27] J. Zhong, Q. Zhong, F. Fan, Y. Zhang, S. Wang, B. Hu, Z. L. Wang, J. Zhou, *Nano Energy* **2013**, *2*, 491 – 497.
[28] S. Wang, L. Lin, Y. Xie, Q. Jing, S. Niu, Z. L. Wang, *Nano Lett.* **2013**, *13*, 2226 – 2233.
[29] G. Åkerlöf, *J. Am. Chem. Soc.* **1932**, *54*, 4125 – 4139.
[30] B. B. Owen, R. C. Miller, C. E. Milner, H. L. Cogan, *J. Phys. Chem.* **1961**, *65*, 2065 – 2070.

Communications

VIP

Contact Electrification

Z.-H. Lin, G. Cheng, L. Lin, S. Lee,
Z. L. Wang* ——— ■■■■–■■■■

Water-Solid Surface Contact Electrification and its Use for Harvesting Liquid Wave Energy

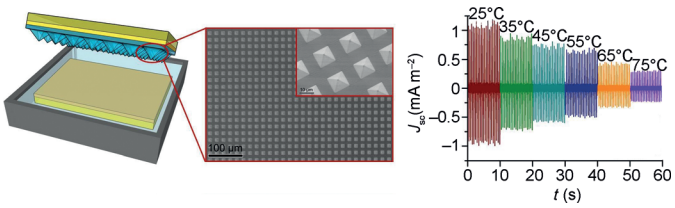

Electrical wave mechanics: A newly designed triboelectric nanogenerator is based on the contact electrification between a patterned polydimethylsiloxane pyramid array and water. Cost-effective and simple, the prototype triboelectric nanogenerator shows the potential to harvest energy from liquid waves and serve as chemical and temperature sensors.